

An H₂O Maser in the Infrared Source IRAS 20126+4104

E. E. Lekht¹, M. I. Pashchenko², and A. M. Tolmachev³

¹*Instituto Nacional de Astrofísica, Óptica y Electrónica,
Luis Enrique Erro No. 1, Apdo Postal 51 y 216, 72840 Tonantzintla, Puebla, México*

²*Sternberg Astronomical Institute, Universitetskii pr. 13, Moscow, 119992 Russia*

³*Pushchino Radio Astronomy Observatory, Astro Space Center of Lebedev Physical Institute,
Russian Academy of Sciences, Pushchino, Moscow oblast', 142290 Russia*

Received October 20, 2006; in final form, December 27, 2006

Abstract—Results of monitoring of H₂O maser in the infrared source IRAS 20126+4104, which is associated with a cool molecular cloud, are presented. The observations were carried out on the 22-meter radio telescope of the Pushchino Radio Astronomy Observatory (Russia) between June 1991 and January 2006. The spectrum of the H₂O maser emission extends from -16.7 to 4.8 km/s and splits into separate groups of emission features. Cyclic variations of the integrated maser flux with a period from 3.4 to 5.5 years were detected, together with strong flares of up to 220 Jy in individual emission features. It is shown that large linewidths in periods of high maser activity are due to small-scale turbulent motions of the material. An expanding envelope around a young star is accepted as a model for the source. The protostar has a small peculiar velocity with respect to the molecular cloud (~ 2 km/s). Individual emission features form organized structures, including multi-link chains.

PACS numbers : 98.58.Ec, 97.10.Bt

DOI: 10.1134/S1063772907070025

1. INTRODUCTION

The source IRAS 20126+4104 is associated with a cool molecular cloud ($T \sim 40$ K) in the intricate Cygnus X complex at a distance of 1.7 kpc from the Sun. The source radiates intensely in the far infrared (1381 Jy at $60 \mu\text{m}$ and 1947 Jy at $100 \mu\text{m}$ [1]). The molecular cloud does not radiate in the continuum and is not observable in the visual [1]. The protostar within the cloud is likewise not observable due to the high extinction in the cloud: the radiation of the protostar is absorbed by gas–dust material, and is reradiated thermally in the far infrared. Wilking et al. [1] observed the cloud in the radio CO line at a velocity of -3.7 km/s. The source is associated with a bipolar outflow, which is extended in the north–south direction and is $20''$ long [2]. CS line emission was detected at almost the same velocity ($V = -3.8$ km/s) [3]. All these features testify that IRAS 20126+4104 is very young.

OH maser emission was detected by Cohen et al. [4] in the 1665-MHz line in right-circular polarization at radial velocities -11.9 and 2.0 km/s with fluxes of 4 and 5.7 Jy, respectively; no emission exceeding 0.2 Jy was observed in left-circular polarization. Later, Pashchenko and Le Squeren [5] found time variations of the OH emission. Between 1988

and 1991, the main and secondary peaks “exchanged places”: their fluxes became 9 and 2.2 Jy. In addition, weak left-polarized emission (0.5 Jy) was detected in the main OH line at 1665 MHz, at a velocity of -4.5 km/s, close to that of the dense molecular cloud (-3.7 km/s in the CO lines [2] and -3.8 km/s in the CS line [3]), as well as weak unpolarized emission (0.3 Jy) in the 1612 MHz satellite line, at a velocity of -10.7 km/s.

Maser emission in the 1.35 cm H₂O line ($F = 45$ Jy) was detected in 1992 at $V_{\text{LSR}} = -4.1$ km/s [5, 6], i.e., at a velocity similarly close to that of the molecular cloud. According to Xiang and Turner [6], the H₂O maser is offset $+5''$ from the center of the IRAS source; thus, the maser should be associated with the bipolar outflow. However, almost at the same time, Tofani et al. [7] showed that the H₂O emission they had detected in 1992 is projected exactly on the IRAS source, and comes from three spots aligned east–west and spread over $0.5''$.

Methanol maser emission is also observed toward IRAS 20126+4104. MacLeod and Gaylard [8] detected a class II methanol maser at two radial velocities: at -6 km/s with a flux of 7 Jy and weaker emission at -8 km/s. A class I methanol maser emits at a velocity of -3.5 km/s [9]. In 1995, Slysh et al. [10]

observed also a symmetric two-peaked emission, but with considerably greater fluxes, about 60 Jy at -7.6 and -6.5 km/s. Later, in 1999, Szymczak et al. [11] observed asymmetric emission at velocities from -8 to -5 km/s with a peak flux of 38 Jy. All this suggests that the methanol maser in IRAS 20126+4104 is strongly variable.

The first results of long-term monitoring of the H_2O maser in a source of a similar type were published for IRAS 06308+0402 [12]. It was shown that the cyclic character of the variability of the H_2O maser emission in this very young object has a period that is appreciably shorter than in masers associated with ordinary, not cool molecular clouds. Is this a rule or an exception?

The current study is devoted to the results of monitoring of the H_2O maser in IRAS 20126+4104 in 1991–2006.

2. OBSERVATIONS AND DATA

Observations of the H_2O maser emission toward the source IRAS 20126+4104 ($\alpha_{1950} = 20^{\text{h}}12^{\text{m}}41^{\text{s}}$, $\delta_{1950} = 41^{\circ}04'20''$) were carried out on the 22-m radio telescope in Pushchino from June 1991 to January 2006. The mean interval between our observations was 2.3 months. The noise temperature of the system with a cooled FET amplifier at the front end was 150–230 K. The receiver upgrade of 2000 decreased the noise temperature to 100–130 K.

The signal was analyzed using a 96-channel (128-channel since July 1997) filter-bank spectrometer with a resolution of 7.5 kHz (0.101 km/s by the radial velocity in the 1.35 cm line); after the end of 2005, a 2048-channel autocorrelator with a resolution of 6 kHz (0.081 km/s) was used. For an unresolved source, an antenna temperature of 1 K corresponds to a flux density of 25 Jy.

Figure 1 presents a catalog of the H_2O spectra. The double arrow shows the scale in Janskys. The horizontal axis is the velocity relative to the Local Standard of Rest. For convenience, baselines are drawn on each spectrum, and all the graphs are plotted on the same scale.

Figure 2a shows a superposition of all the spectra, except for those without detectable emission. The spectrum can be separated into intervals in which emission features are concentrated: -16.5 to -12.5 , -12.5 to -3.4 , -3.4 to 1.0 , and 1.0 to 4.8 km/s. The vertical bars denote boundaries between these intervals, labeled *a*, *b*, *c*, and *d*, respectively. Throughout the 15-year monitoring, we observed weak emission with a flux not more than 15 Jy at the boundary between intervals *b* and *c* (1991, 2001, and 2004). At all other epochs, the fluxes between groups of features

did not exceed 6–8 Jy. The solid arrows show the positions of methanol emission features [8], which coincide with the position of the most intense H_2O maser emission; the dotted arrows shows the positions of 1665-MHz hydroxyl maser peaks [5].

The horizontal bars in Fig. 2b show for each spectrum radial-velocity intervals in which H_2O maser emission was observed. Note that the maser activity moved with time from one group of emission features to another. The positions of the emission peaks are marked with open circles. The observed drift of the maser activity was ordered rather than chaotic, and is fairly well described by a polynomial fit (dotted curve in Fig. 2b). The main H_2O emission peaks are numbered in the order of their appearance.

To find the parameters of the cyclic maser variability, we calculated the integrated flux (F_{int}) for each spectrum. Figure 3 presents a plot of the variations of F_{int} . There is a pronounced alternation of maxima and minima of F_{int} . The time intervals between the successive maxima 1–4 are 4.6, 5.5, and 3.4 years.

We separated the spectrum into individual components using Gaussian fitting. In many spectra, the emission was faint, and we cannot guarantee completeness for components with fluxes below 4–5 Jy or in the case of strong blending. Figure 4 shows a representation of the H_2O spectra as individual components for 1991–2006. We have included the data of Tofani et al. [7] (open circles). The dash-dotted line shows the central velocity of the H_2O maser. The dashed lines reflect trends in the drift of the emission of individual features, as well as of large groups of features (spectrum intervals *b*, *c*, and *d*). All are numbered. The radial velocities of the emission of other molecules are given at the right (Table 2, column 4).

Note the asymmetric arrangement of the components relative to the central velocity of the H_2O maser; the character of the asymmetry changed appreciably with time.

3. DISCUSSION

The water maser toward IRAS 20126+4104 has become the third source associated with a dense, cool molecular cloud for which long-term monitoring has been carried out. Observations with high angular resolution [7] and the results of long-term monitoring (this paper) enable us to qualitatively assess a scenario for the maser source in which a star forms at a very early evolutionary stage and is embedded in a cool molecular cloud.

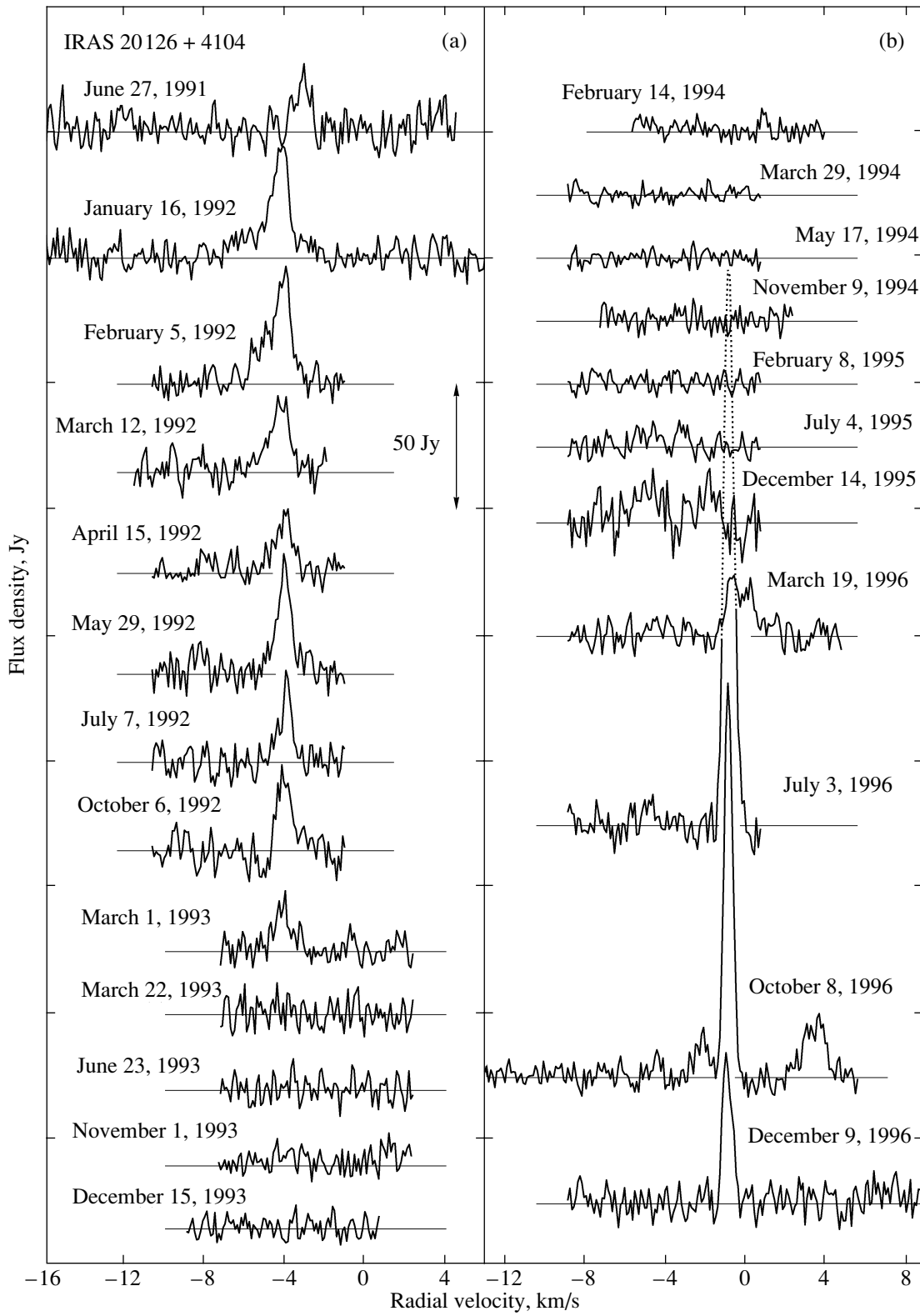


Fig. 1. A catalog of H₂O spectra of IRAS 20126+4104.

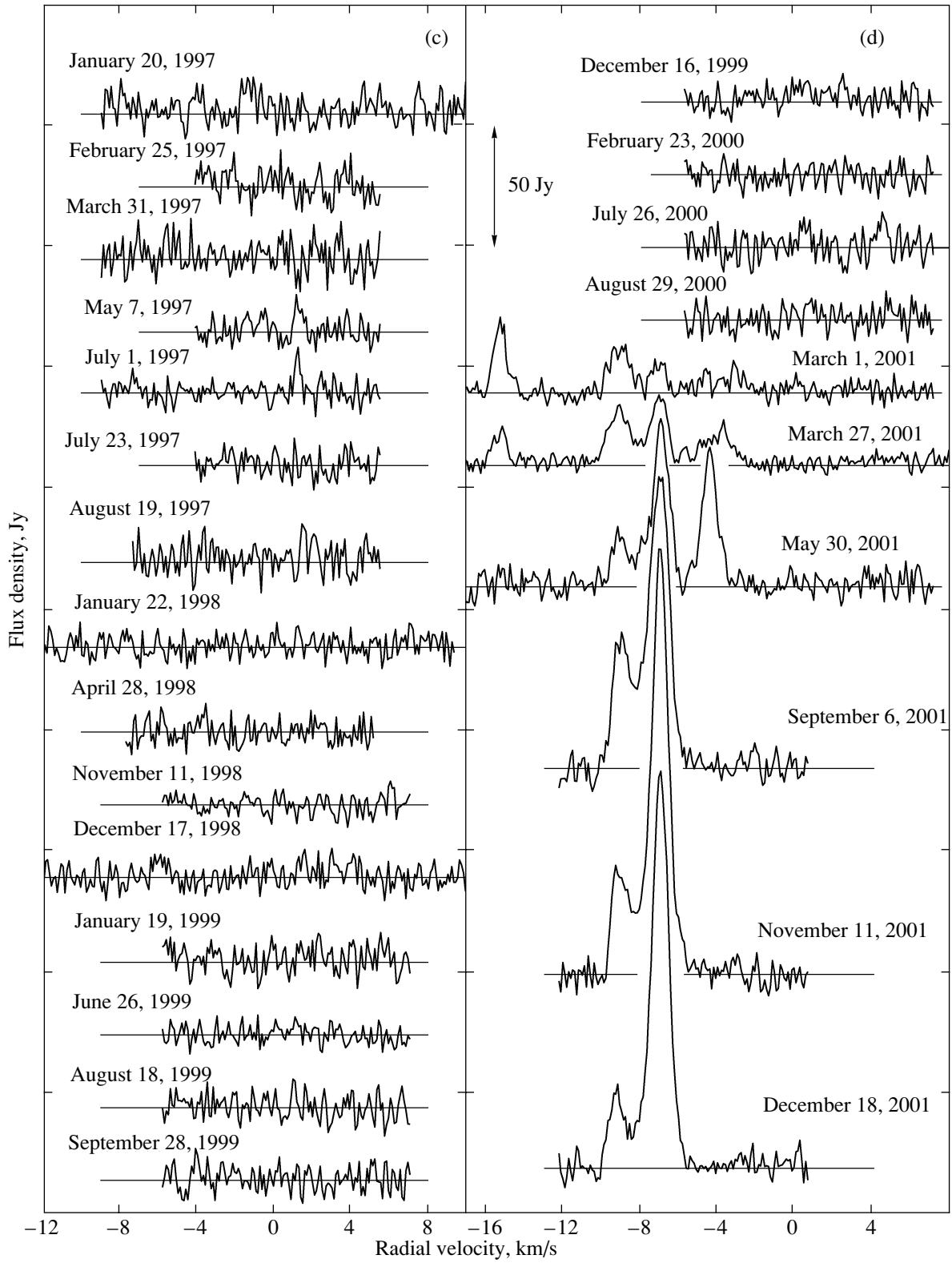


Fig. 1. (Contd.)

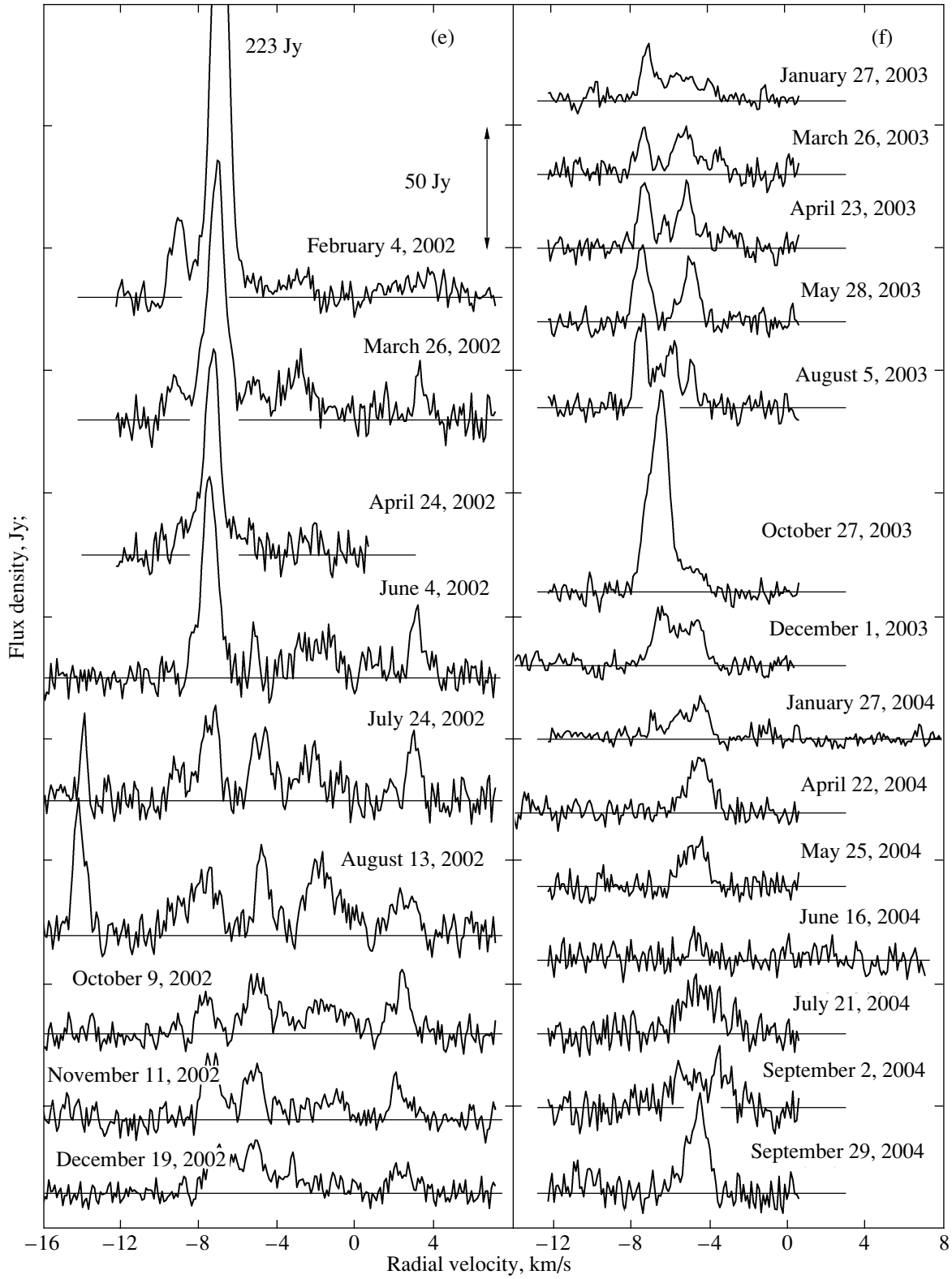


Fig. 1. (Contd.)

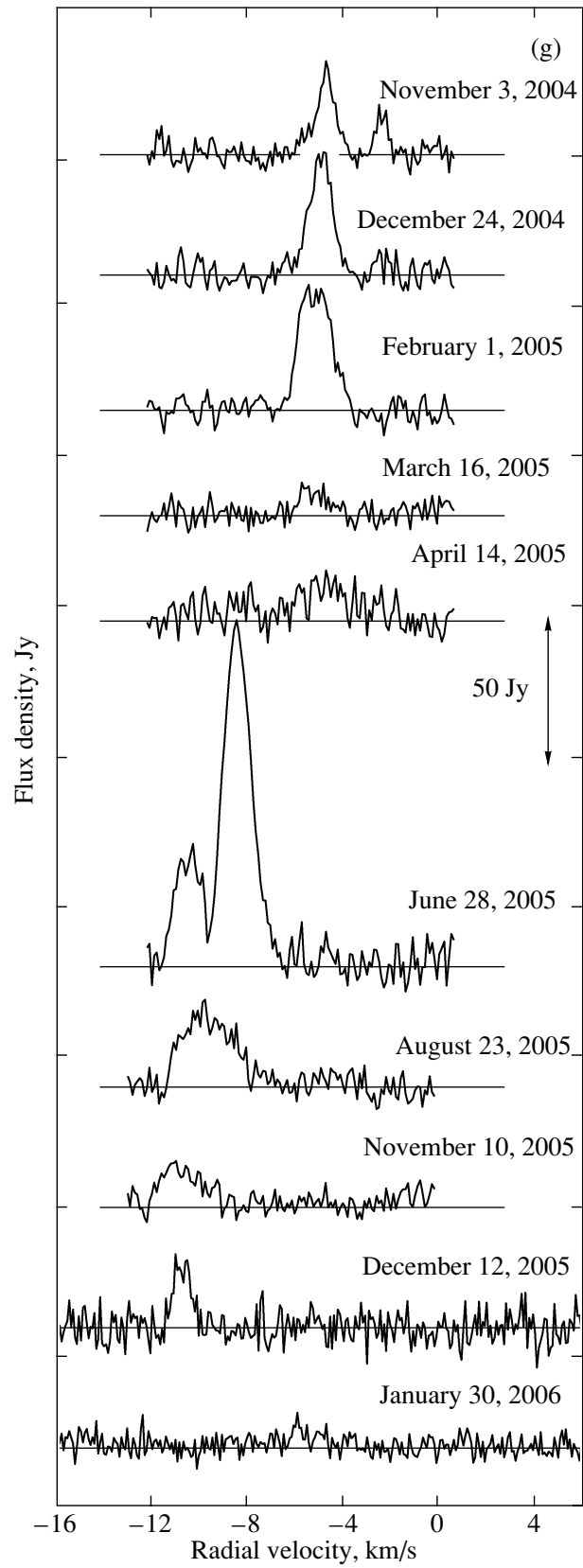


Fig. 1. (Contd.)

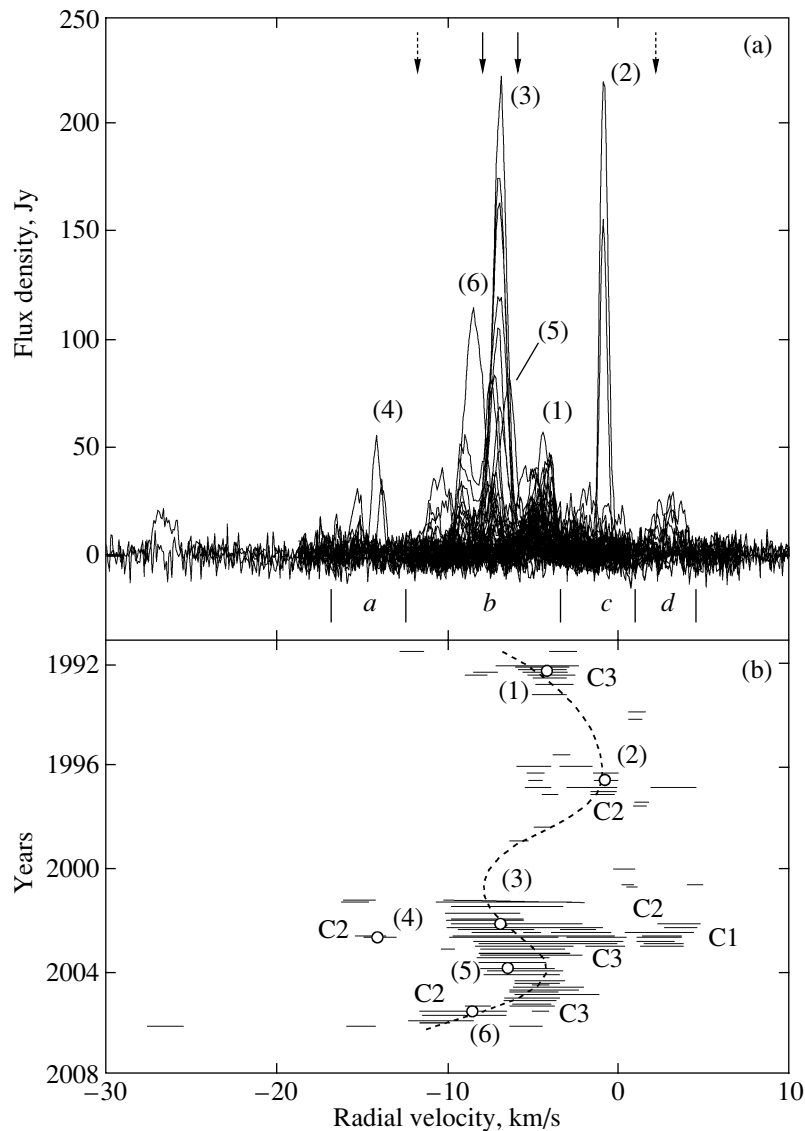


Fig. 2. Superpositions of (a) the H₂O spectra for 1991–2006 and (b) the V_{LSR} intervals (horizontal bars) in which maser emission was observed. Spectra without detectable emission are not included. The vertical bars show the boundaries of individual spectral groups. The positions of maser peaks are shown with solid (methanol) and dotted (hydroxyl) arrows at the top. The main H₂O peaks are numbered in the order of their appearance. The positions of the peaks are shown with open circles. The dotted curve shows a fitted polynomial. The labels C1, C2, and C3 denote the identified emission features (see text for details).

3.1. Analysis of the Catalog of H₂O Spectra

Our monitoring of the H₂O maser in IRAS 20126+4104 began in June 1991; we detected emission at two radial velocities: -3.1 km/s with a flux of 20 Jy and -12 km/s with a flux of 8 Jy. Follow-up observations of 1992 showed that strong emission at -4.3 km/s, with a peak flux exceeding 50 Jy. This is consistent with the results of publications reporting the discovery of the H₂O maser in IRAS 20126+4104, which was observed in April [6] and November [7] 1992.

Our monitoring shows that the maser emission varied very strongly, from a flux of 223 Jy to its complete disappearance. We observed several flares at different radial velocities, which were consequences of enhanced activity of the maser as a whole. Sometimes, short-lived flares of more or less isolated emission features with fluxes from 25 to 115 Jy occurred in the entire radial-velocity range from -15.5 to 3.5 km/s. The linewidths of the emission features during flares are listed in Table 1. Column 2 contains the V_{LSR} intervals of the studied features; columns 3 and 4 list intervals of the linewidths and

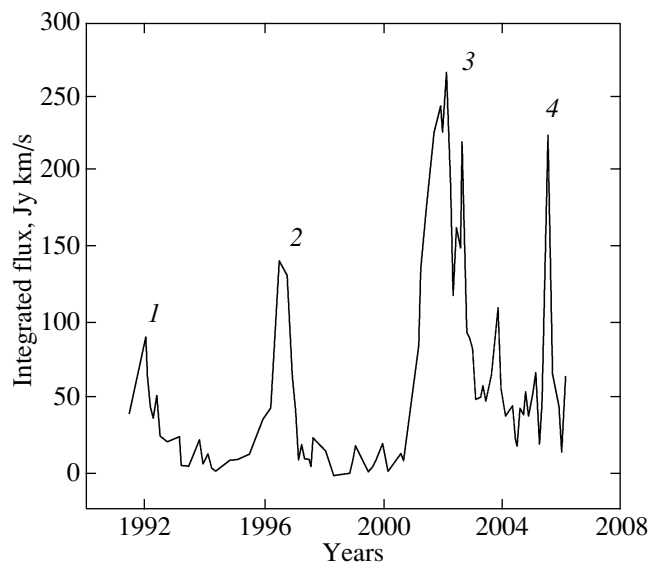


Fig. 3. Variations of the integrated flux. The intervals between successive emission maxima 1–4 are 4.6, 5.5, and 3.4 years.

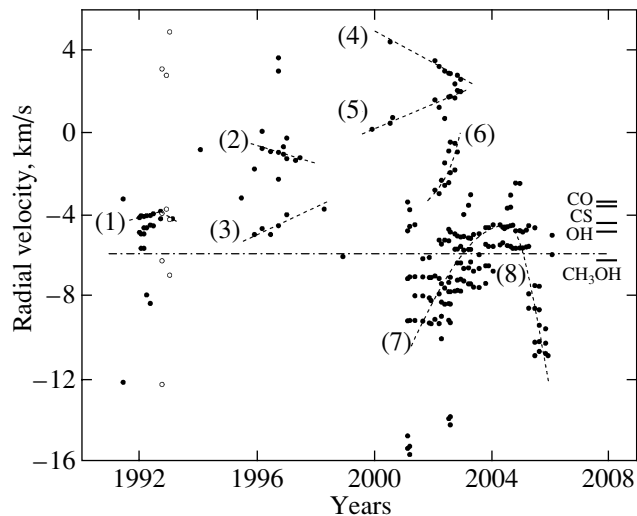


Fig. 4. Separation of the H_2O spectra into individual components (see text for details).

peak fluxes, respectively. The strong emission in 2005 has a fairly symmetric line shape, though it is very broad (1.3 km/s). Only the right-hand wing of the line contains a component that is an order of magnitude weaker than the main peak. After eliminating this component, the line shape does not differ significantly from a Gaussian. It is most likely that, in this case, we have a broad single line, rather than a superposition of several narrower lines.

We find no triplet structure in the spectra, though there are two groups of isolated features at the ends of the spectrum. However, their emission is rather weak relative to that in the velocity interval from -12.5 to 1 km/s, and appeared only occasionally.

3.2. Cyclic Activity of the H_2O Maser

We used the integrated maser flux to assess the activity of the maser as a whole, as a system of maser spots with a single activity center. According to our monitoring, during long time intervals, the H_2O spectra had rather faint emission. To avoid large errors in calculating the integrated flux, we carefully corrected the zero (base) line of each spectrum. After this correction, we plotted a curve of the integrated-flux variations, shown in Fig. 3. We observe four maxima and deep minima, which reach the zero level. The most complex activity cycles were 3 and 4, which were accompanied by rapid rises and sharp decays

Table 1. Main parameters of individual H₂O emission features in IRAS 20126+4104

Years	V_{LSR} interval, km/s		Linewidth, km/s	Flux density (min/max), Jy
1	2		3	4
1992	-5.5	-3.2	0.45–0.65	40/70
1996	-1.5	0.6	0.4–0.6	20/200
2001–2002	-10.0	-3.5	0.8–1.0	22/223
2002	-14.5	-13.5	0.4–0.5	25/50
2003	-8.0	-5.5	0.7–0.8	25/80
2005	-9.6	-7.0	1.3	115

in the emission of the main peaks; these cycles had rather extended spectra.

Thus, the H₂O maser variability was cyclic with periods ~ 4.6 , 5.5, and 3.4 years. This may reflect the quasi-periodic character of the variability of a young star at the stage of its formation. The obtained variability periods are only a factor of two to three shorter than those found for masers in star-forming regions associated with ordinary molecular clouds.

3.3. Individual Emission Features

Analysis of the spectrum's structure—i.e., isolation of individual spectral components and tracing their evolution—is also important in constructing a model of the maser. Each component is identified either with a separate maser spot or with a compact cluster of spots.

We found in the maser associated with IRAS 20126+4104 many more emission features than in the H₂O maser in IRAS 06308+0402 (Fig. 4). Most features drift in V_{LSR} . In some cases, this drift is real, e.g., for components (1), (2), and (4). The existence of a drift at a velocity of -4 km/s also follows from the paper of Tofani et al. [7]. In other cases, the apparent shift of the emission peaks in the spectra is due to a change in the ratio of the intensities of two or more features at similar velocities. This was especially conspicuous in 2001–2004.

We identified another type of the drift manifest as a tendency for a shift in the activity in V_{LSR} . This occurred during a high level of the maser emission. The emission of some features lagged relative to that of others. This drift pattern was fairly regular, as is shown in Fig. 4 by the dashed lines (6), (7), and (8). Based on all this, we suppose that the maser spots are not arranged chaotically and form organized structures, e.g., chains.

The different direction of the drift of structures (7) and (8) in the third and fourth activity cycles can be

explained if they belong to different clusters of maser spots. According to our identification, the group of spots (7) is associated with C3, and group (8) with C2 [7].

3.4. A Model for the H₂O Maser in IRAS 20126+4104

According to Tofani et al. [7], there are three clusters of maser spots (called three spots in [7])—C1, C2, and C3—toward IRAS 20126+4104. Though these observations were made in the initial period of our monitoring, we have attempted to identify the main flares by extrapolating the monitoring data. We have also taken into account that, according to Tofani et al. [7], the emission in spectral intervals *a* and *d* (Fig. 2a) belongs to cluster C2. Furthermore, we have taken into consideration the existence of correlations between different spectral intervals. For instance, the emission at -9.2 and -7 km/s was correlated in the third activity cycle (2001). The results of our assigning the emission features to the spots C1, C2, and C3 in accordance with our criteria are shown in Fig. 2b by the designations C1, C2, and C3.

For a better understanding of the structure of the maser emission toward IRAS 20126+4104, we compiled Table 2, which lists some parameters of the emission of the molecular cloud in the ¹²CO and CS lines, as well as in the methanol, hydroxyl, and water masers. In column 2, the labels R and L for the 1665-MHz line denote right- and left-circular polarization, respectively. In column 3, in the case of a single line, we took its linewidth and, in the case of two-peaked or more complex spectra, we took the velocities of the features at the ends of the spectrum.

There is good coincidence of the central velocities in the maser sources with the velocity of the molecular clouds in which the masers are embedded together with the source of their excitation, a protostar. The maximum difference of the central velocities of the maser emission from the cloud velocity only slightly

Table 2. Main parameters of molecular emission in IRAS 20126+4104

Molecule	Frequency, MHz	Velocity interval, km/s	Central velocity, km/s	Reference
1	2	3	4	5
^{12}CO	230		-3.7	[2]
CS	97.98	3.2	-3.8	[3]
CH ₃ OH	6668	-7.5/-5.5	-6.5	[8]
	6668	-8/-4	-6	[9, 10]
OH	1665R	-11.9/2	-4.95	[4]
	1665R	-11.9/2.2	-4.85	[5]
	1665L	~1	-4.6	[5]
	1612	-10.7	-	[5]
H ₂ O	22 235	-16.5/4.8	-5.85	This paper

exceeds 2 km/s (methanol and water). The H₂O maser monitoring gives the most comprehensive picture of the number of maser spots and the total velocity range of the emission. Therefore, the central velocity, -5.85 km/s, can be taken as the velocity of the system and, hence, of the protostar. In this case, the line-of-sight component of the system's peculiar velocity is $V_{\text{CO}} - V_{\text{H}_2\text{O}} \approx 2$ km/s.

Hence we can see that there is virtually no peculiar motion of the protostar relative to the molecular cloud within the thermal linewidth, which can also be increased by small-scale turbulent motions of the material ($\Delta V = \sqrt{\Delta V_{\text{therm}}^2 + \Delta V_{\text{turb}}^2}$). According to Wilking et al. [2], the velocity dispersion found from the ^{12}CO line is ≈ 4 –5 km/s.

The maser spots C1, C2, and C3 (the H₂O maser) are aligned orthogonal to the bipolar outflow within 0.5'' [7], i.e., 1.5×10^{16} cm (for a distance to IRAS 40126+4104 of 1.7 kpc). The absence of a triplet structure in the spectrum may favor a model with an expanding envelope that hosts the maser spots.

The methanol and hydroxyl masers have a fairly simple spectral structure. They are probably associated with larger scale masing regions than the H₂O spot groups. Most likely, the OH maser at 1665 MHz (right-circular polarization) is spatially identified with C2 and the left-circularly polarized maser with C3. In the expanding envelope model, emission peaks at the ends of the OH spectra at $V_{\text{LSR}} = -11.9$ and 2.2 km/s should come from the near (approaching) and far (receding) parts of the envelope, respectively.

Note that the three spots (C1, C2, and C3) in IRAS 20126+4104 were detected in a period of low maser activity [7]. Our monitoring has shown that,

at some epochs, the maser activity is high and the emission is observed in a broad V_{LSR} interval. It may be that, at these epochs, the emission comes, not from three maser spots (clusters of spots), but from a greater number of spots between C1 and C3. However, these are not manifest at lower activity levels.

Finally, we have found that the linewidths of individual spectral features depend on the activity of the maser as a whole: the higher the activity, the broader the lines. Narrow lines (0.4–0.6 km/s) in a period of high maser activity (2002) were observed only at velocities from -16 to -13 km/s. At the remaining epochs, we observed no emission at all there. The line broadening may be due to the fact that, at higher maser activity levels, i.e., with higher levels of pumping, the sizes of the regions (spots) responsible for this emission increase. If small-scale turbulent motions exist in the medium hosting the maser spots, the role of turbulence in the line formation increases, resulting in the observed line broadening.

The observed shift of the activity peaks, which is well described by a polynomial fit (Fig. 2), cannot be explained by cyclic variability of the star alone. It is quite possible that the observed phenomenon is also due to the structure of the envelope, i.e., to the arrangement of the maser spots. Certainly, however, this cannot be the only origin. The model can be refined by observations with high angular resolution during periods of sufficiently high maser activity.

4. MAIN RESULTS

Let us list the main results of our 15-year monitoring of the water maser in IRAS 20126+4104, associated with a cool molecular cloud.

(1) We have presented a catalog of spectra of the H₂O maser emission in the 1.35-cm line toward the infrared source IRAS 20126+4104, associated with a cool molecular cloud, for the period from June 1991 to January 2006 (Fig. 1) with a mean interval between observations of about 2.3 months. The spectral resolution in radial velocity was 0.101 km/s.

(2) The H₂O maser emission is observed in the V_{LSR} interval from -16.7 to 4.8 km/s and is split into groups of features occupying velocities from -16.7 to -12.5 , -12.5 to -3.4 , -3.4 to 1.0 , and 1.0 to 4.8 km/s (Fig. 2a). The central velocity, equal to -5.85 km/s, differs from that of the CO cloud by only ≈ 2 km/s.

(3) We have found cyclicity in the maser activity (four cycles) with intervals between successive maxima of 4.6, 5.5, and 3.4 years (Fig. 3). This is a factor of two to three shorter than the durations of the quasi-periods in H₂O masers that are not associated with cool molecular clouds. During the periods of the highest maser activity (cycle 3), the spectra were most extended and emission was observed from all the groups of emission features (Fig. 2). In these periods, line broadening could be due to small-scale turbulent motions of the material in the maser regions.

(4) We favor model with an expanding envelope that contains, in addition to the known and identified maser regions C1, C2, and C3, at least one (possibly, several) other region of maser emission. The individual emission features may form ordered structures, e.g., multi-link chains. The central star has a small peculiar velocity with respect to the molecular cloud (~ 2 km/s). We can explain also explain the structure of the hydroxyl maser in the framework of this model.

ACKNOWLEDGMENTS

The RT-22 radio telescope is supported by the Ministry of Education and Science of the Russian

Federation (facility registration number 01-10). This work was supported by the Russian Foundation for Basic Research (project no. 06-02-16806). The authors are grateful to the staff of the Pushchino Radio Astronomy Observatory for help with the observations.

REFERENCES

1. B. A. Wilking, L. G. Mundy, J. H. Blackwell, and J. E. Howe, *Astrophys. J.* **345**, 257 (1989).
2. B. A. Wilking, J. H. Blackwell, and L. G. Mundy, *Astron. J.* **100**, 758 (1990).
3. L. Bronfman, L. A. Nyman, and J. May, *Astron. Astrophys., Suppl. Ser.* **115**, 81 (1996).
4. R. J. Cohen, E. E. Baart, and J. L. Jonas, *Mon. Not. R. Astron. Soc.* **231**, 205 (1986).
5. M. I. Pashchenko and A. M. Le Squeren, *Pis'ma Astron. Zh.* **20**, 85 (1994) [*Astron. Lett.* **20**, 69 (1994)].
6. D. Xiang and B. E. Turner, *Astrophys. J., Suppl. Ser.* **99**, 121 (1995).
7. G. Tofani, M. Felli, G. B. Taylor, and T. R. Hunter, *Astron. Astrophys., Suppl. Ser.* **112**, 299 (1995).
8. G. C. MacLeod and M. J. Gaylard, *Mon. Not. R. Astron. Soc.* **256**, 519 (1992).
9. S. Kurtz, P. Hofner, and C. V. Alvarez, *Astrophys. J., Suppl. Ser.* **139**, 257 (1999).
10. V. I. Slysh, I. E. Val'ts, S. V. Kalenskii, et al., *Astron. Astrophys., Suppl. Ser.* **134**, 115 (1999).
11. M. Szymczak, G. Hrynek, and A. J. Kus, *Astron. Astrophys., Suppl. Ser.* **143**, 269 (2000).
12. M. I. Pashechenko, E. E. Lekht, and A. M. Tolmachev, *Pis'ma Astron. Zh.* **29**, 823 (2003) [*Astron. Lett.* **29**, 731 (2003)].

Translated by G. Rudnitskii